ANALYTICAL STUDY OF STABILITY OF WING ROCK MODELS

Entz, R.M.U , Correa, L.G.N. , Marques, F.D. , Catalano, F.M. , Cosin, R.
Engineering School of São Carlos – University of São Paulo, Brazil

Keywords: *wing rock, stability criterion, non-linear dynamics, flight mechanics, energy model*

Abstract

Slender wings and some wing-body configurations are capable of producing vortex lift at higher angles of attack. This seemingly beneficial feature is however susceptible to wing rock - a non-linear phenomenon that can cause the airplane to reach a limit-cycle oscillation due to vortex asymmetry. Some stability models were developed to predict and control the wing rock. In the present work, an analytical investigation of wing rock dynamics leads to a stability criterion, which can be applied for both open and closed loop systems, determining boundaries for the existence of the non-linear phenomenon.

1 Introduction

Wing rock occurs in slender wings and some wing-body configurations. This phenomenon is a side effect of vortex lift, that is present under some specific flight conditions, when asymmetry arises in the lifting vortex structure, leading to a limit cycle oscillation in roll [1]. This movement can then couple with other axis movements [2] and can cause loss of control of the airplane. As this phenomenon occurs at landing and flight maneuvers, wing rock is a dangerous situation and also a major problem during the tracking of an enemy target, particularly for fighters, such as the F-5 [3], F-8 [4] and F-15 [5].

This phenomenon has been motivating a series of research studies proposing non-linear models for its prediction, in the other hand the literature provides mainly empirical or semi-empirical formulations due to the complexity associated with the modeling of the flow field [6]. In wing rock investigation, the stability analysis is an issue of great interest that will be treated in this work.

The present investigation makes use of a simplified, semi-empirical model for rolling motion and proposes a method for the analysis of their stability both on open loop and feedback-controlled cases.

2 Methodology

2.1 Model Analysis

Several semi-empirical formulations have been proposed to simulate the characteristic roll motion of wing rock. The relation used as an example is adapted from [7] and relies on the common assumption that the roll moment coefficient C_l is a function of the roll angle Φ and its first derivative

$$C_l = a_1\Phi + a_2\dot{\Phi} + a_3|\Phi|\dot{\Phi} + a_4\frac{\dot{\Phi}}{|\dot{\Phi}|} \quad , \qquad \lim_{t\to 0}\frac{\dot{\Phi}}{|\dot{\Phi}|} = 0 \quad , \tag{1}$$

where a_1 to a_4 are real-valued coefficients obtained in a semi-empirical context.

The development of the equation of motion then is based on the aerodynamic relation for the roll moment, that is,

$$L = qSbC_l \quad . \tag{2}$$

Using Newton's second law, it becomes

$$\ddot{\Phi} - a_1 \frac{qSb}{I_{xx}}\Phi - a_2 \frac{qSb}{I_{xx}}\dot{\Phi} - a_3 \frac{qSb}{I_{xx}}|\Phi|\dot{\Phi} - a_4 \frac{qSb}{I_{xx}} \frac{\dot{\Phi}}{|\dot{\Phi}|} = 0 \quad . \tag{3}$$

The analytical description of the system is not possible due to the two non-linear terms a_3 and a_4. However the analysis of some limit cases can help the understanding of some general characteristics of the system.

The first case analyzed is the linear system, when the values of a_3 and a_4 are zero. For this first particular case, it is possible to use the relations for second order, linear time-invariant systems and determine the natural frequency of oscillation and the damping coefficient as

$$\begin{aligned} \omega_n &= (-a_1)^{1/2} \left(\frac{qSb}{I_x x} \right)^{1/2} \quad , \\ \zeta &= \frac{-a_2}{2(-a_1)^{1/2}} \left(\frac{qSb}{I_x x} \right)^{1/2} \quad . \end{aligned} \tag{4}$$

This first case is then compared to the second case, in which only the value of a_4 is assumed to be zero. The equation of motion results,

$$\ddot{\Phi} - a_1 \frac{qSb}{I_{xx}}\Phi + \left(-a_2 \frac{qSb}{I_{xx}} - a_3 \frac{qSb}{I_{xx}}|\Phi| \right) \dot{\Phi} = 0 \quad . \tag{5}$$

Eq. (5) was written in a form that is analogous to the LTI (linear time-invariant) system, and for analysis purposes only it is compared with its equation, allowing the determination of pseudo values for the natural frequency and damping, that is,

$$\begin{aligned} \tilde{\omega}_n &= (-a_1)^{1/2} \left(\frac{qSb}{I_x x} \right)^{1/2} \quad , \\ \tilde{\zeta} &= \frac{-a_2 - a_3|\Phi|}{2(-a_1)^{1/2}} \left(\frac{qSb}{I_x x} \right)^{1/2} \quad . \end{aligned} \tag{6}$$

One conclusion that can be drawn from this development is that, for sufficiently small non-linearities, the natural frequency of the oscillation of the non-linear system is roughly the same of the LTI system. This assumption plays a critical role in the development of the method.

The damping equation is used whenever the original relation is applied for model-fitting. To proceed with the analysis, it is assumed that the system suffers an infinitesimal perturbation ε_Φ is amplified if, and only if $\tilde{\zeta} < 0$. Assuming that,

$$\lim_{t \to 0} |\Phi| = 0 \Rightarrow \lim_{t \to 0} \tilde{\zeta} = \zeta \quad , \tag{7}$$

one can conclude that,

$$\zeta < 0 \Rightarrow a_2 > 0 \quad , \tag{8}$$

for the amplification of an infinitesimal perturbation, which could lead to an oscillation of infinite amplitude, as in a LTI system.

However, this can be avoided in the model by making $a_3 < 0$. So one can conclude that at some amplitude the amplification turns to zero. This analysis can be used for preliminary experimental data fitting by following the suggested procedure:

- calculate a_1 according to the LCO (limit-cycle oscillation) frequency
- set a_2 according to the amplification ratio observed
- adjust a_3 to achieve the LCO amplitude

The fourth term in the Eq. (3) is not analyzed at the moment. This can represent a Coulomb friction-like effect or some kind of on-off controller that reacts for or against the sense of the angular speed. This term, however, will be used further in the development of the work.

2.2 An energy approach

The system analysis by energy requires manipulation from Eq. (2), which represents the roll moment of the aircraft. From the definition of work,

$$W = \int_{t_1}^{t_2} L d\Phi \quad , \tag{9}$$

this relation is then used to determine the gain or loss of mechanical energy, dE, in the system during a cycle [8].

To compute the work from Eq. (9), it is necessary to determine the angular position of the aircraft with relation to time. For the wing rock phenomenon it can be written in the form,

$$\Phi(t) = A \cdot f(t) \cdot cos(\omega t) \quad . \tag{10}$$

This generic form is not adequate for integration, as the function that represents the amplification envelope is not previously known. One reasonable simplification considers the system in a limit-cycle, and $f(t) \equiv 1 \quad \therefore \quad \Phi(t) = Asin(\omega t)$.

This allows Eq. (9) to be written as,

$$dE = \int_{t_1}^{t_2} LA\omega cos(\omega t)\, dt \quad . \tag{11}$$

As stated in the last section, the LCO frequency is assumed the same as that of the equivalent LTI system. The Eq. (11) can then be rewritten as,

$$dE = \int_{0}^{2\pi/\omega_n} LA\omega_n cos(\omega_n t)\, dt \quad . \tag{12}$$

In order to perform this integral analytically using the expression given in Eq. (1), it is necessary to break down the cycle into four parts, as the non-linear terms have kinks and discontinuities, that is

$$dE = W_1 + W_2 + W_3 + W_4 \quad , \tag{13}$$

where

$$\begin{aligned}
W_1 &= \int_0^{2\pi/\omega_n} \hat{a}_1 A^2 \omega_n sin(\omega_n t) cos(\omega_n t)\, dt \\
W_2 &= \int_0^{2\pi/\omega_n} \hat{a}_2 A^2 \omega_n^2 cos^2(\omega_n t)\, dt \\
W_3 &= \int_0^{\pi/\omega_n} \hat{a}_3 A^3 \omega_n^2 |sin(\omega_n t)| cos^2(\omega_n t)\, dt \\
&\quad + \int_{\pi/\omega_n}^{2\pi/\omega_n} \hat{a}_3 A^3 \omega_n^2 |sin(\omega_n t)| cos^2(\omega_n t)\, dt \\
W_4 &= \int_0^{\pi/2\omega_n} \hat{a}_4 (-1) A \omega_n cos(\omega_n t)\, dt \\
&\quad + \int_{\pi/2\omega_n}^{3\pi/2\omega_n} \hat{a}_4 A \omega_n cos(\omega_n t)\, dt \\
&\quad + \int_{3\pi/2\omega_n}^{2\pi/\omega_n} \hat{a}_4 (-1) A \omega_n cos(\omega_n t)\, dt \quad ,
\end{aligned} \tag{14}$$

where $\hat{a}_i = a_i \frac{qSb}{I_{xx}}$.

It is important to note that the first term does not contribute to the final value of the integral. This is a necessary conclusion that will be exploited later on.

The integral is greatly simplified to,

$$dE = \frac{4}{3}\hat{a}_3 \omega_n A^3 + \pi \hat{a}_2 \omega_n A^2 + 4\hat{a}_4 A \quad . \tag{15}$$

3 Validation

Assuming the dynamic model of Eq. (1), the following $\hat{a}$ parameters are used in order to simulate the behavior of an airplane in wing rock motion.

$$\begin{aligned}
\hat{a}_1 &= -0.8028 \\
\hat{a}_2 &= +0.0803 \\
\hat{a}_3 &= -0.2141 \\
\hat{a}_4 &= -0.0080
\end{aligned} \tag{16}$$

The time response of the system to an initial perturbation of 15 degrees shows the amplification of the oscillation up to the establishment of a LCO at about 40 degrees (0.7056 rad). It is possible to notice that the overall behavior of the system compares fairly well to the general phenomenon - amplification of an initial perturbation up to the establishment of a sinusoidal oscillation.

With this representative system one now can use Eq. (15). The application of this relation is firstly used in order to find the neutral points, defined as the amplitudes in which there is no energy gain or loss, mathematically

$$dE = 0 \quad . \tag{17}$$

This relation still needs the determination of the natural frequency. There are two possible approaches, the first is the measurement from the LCO and the second is the use of Eq. (4). The second approach is preferred in order to verify the validity of the assumption that $\tilde{\omega}_n \approx \omega_n$.

$$\begin{aligned}
\omega_n &= (-a_1)^{1/2} \left(\frac{qSb}{I_x x}\right)^{1/2} \\
&= \sqrt{-\hat{a}} = 0.8960 rad/s
\end{aligned} \tag{18}$$

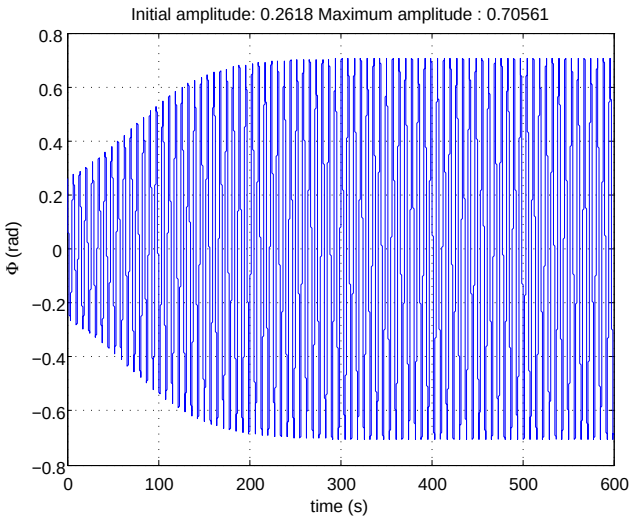

Fig. 1 Time response of the system with an initial perturbation of 15°

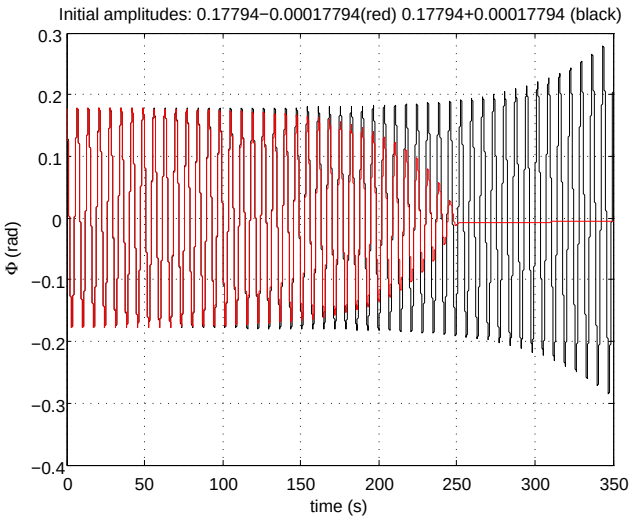

Fig. 2 Simulations around second root, showing the limits of the attenuation region

Solving the Eq. (15), three corresponding roots are obtained, that is,

$$\begin{aligned} A_0 &= 0 \\ A_1 &= 0.1779 \\ A_2 &= 0.7056 \end{aligned} \tag{19}$$

Accordingly to the theory, there are three points where the cycle amplitude is kept. The first root represents the trivial solution when the system is not moving. And the third root represents the LCO amplitude. Comparing the amplitudes from the simulation and the theory one determines that the difference is in order of 10^{-4} in this case, what is considered extremely precise and shows that the hypothesis assumed for the solution are valid for this case.

From an analysis of Eq. (15), it is natural to conclude that the existence of the intermediate root, which defines the critical initial perturbation, is dependent on the condition that $a_4 > 0$.

3.1 The effect of a discontinuous non-linearity

The final validation case was created to push the method to its limits and test the validity of its assumptions. The setup is made to increase the ratio between non-linear and linear terms magnitudes, the chosen values for the terms are

$$\begin{aligned} \hat{a}_1 &= -0.8028 \\ \hat{a}_2 &= +0.8028 \\ \hat{a}_3 &= -1.6056 \\ \hat{a}_4 &= -0.0803 \end{aligned} \tag{20}$$

For this case, it is possible to notice a considerable distortion on the LCO as shown in Figure. This clearly violates the hypothesis applied in Eq. (10), what would render the methodology useless.

It is important to apply the procedure as done previously to test the limitations of the theory. With that, one obtains

$$\begin{aligned} A_0 &= 0 \\ A_1 &= 0.1653 \\ A_2 &= 1.0128 \end{aligned} \tag{21}$$

Surprisingly, the LCO amplitude prediction is fairly precise, with an error of only 0.07%. This result was found on similar cases simulated during this work, but the authors have no conclusive explanation of this unexpected agreement between the prediction and the simulation. However, it is important to notice that there is a con-

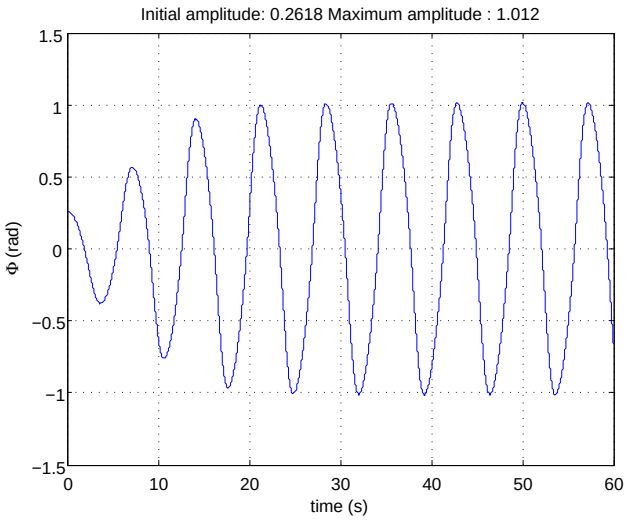

Fig. 3 Oscillation build-up on system with stronger non-linearities. Note that the oscillation shape deviates from that of a sinus, going against the assumptions of the methodology

siderable difference between the value of the second root and the observed critical initial perturbation. For this case, it was found that the critical initial value is $0.1775 rad$, which means a discrepancy of about 7%. The only conclusion that can be drawn from this case is that this methodology should not be used with such cases, with the risk of getting arbitrarily imprecise results.

4 Application

It is possible to analyze the behavior of the system in a closed loop, assuming the following control law

$$\delta_a = k_1\Phi + k_2\dot{\Phi} + k_3\dot{\Phi}|\Phi| + k_4\frac{\dot{\Phi}}{\ddot{\Phi}} \quad . \tag{22}$$

Considering that the aileron deflection produces a linear effect in the roll moment coefficient, proportional to $C_{l_{\delta_a}}$, the equation of motion becomes

$$\begin{aligned}&\ddot{\Phi} - (\hat{a}_1 + \tilde{k}_1)\Phi - (\hat{a}_2 + \tilde{k}_2)\dot{\Phi} \\ &- (\hat{a}_3 + \tilde{k}_3)|\Phi|\dot{\Phi} - (\hat{a}_4 + \tilde{k}_4)\frac{\dot{\Phi}}{|\dot{\Phi}|} = 0 \quad ,\end{aligned} \tag{23}$$

where

$$\tilde{k}_i = k_i\frac{C_{l_{\delta_a}} qSb}{I_{xx}} \quad .$$

The first important conclusion comes from Eq. (14), which shows that the value of $\tilde{k}_1$ does not play a significant role on the problem stability, as the integration of its term yields zero. This condition is not verified in the 6DoF model, mainly because the fitting does not take into account the changes in ω_n that the eventual insertion of a $\tilde{k}_1$ gain brings. This is considered a limitation in this methodology and it must be taken into account.

In the other hand, from equation Eq. (15) it is possible to conclude that, in order to always have $dE < 0$, it is necessary to obey the condition,

$$A < \frac{3\pi}{4}\frac{\hat{a}_2 + \tilde{k}_2}{\hat{a}_3 + \tilde{k}_3} \tag{24}$$

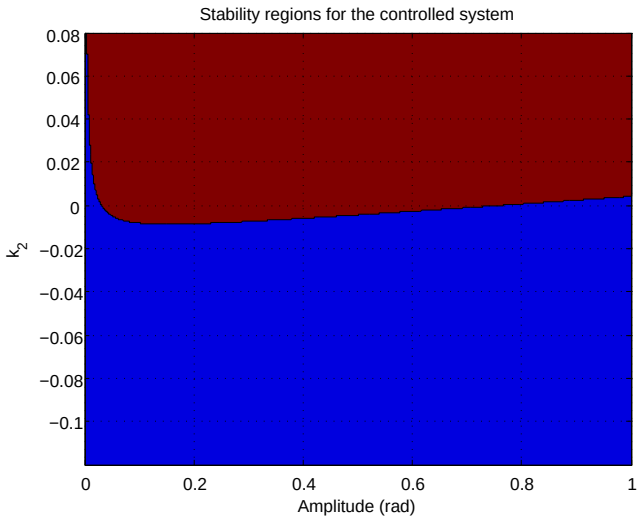

Fig. 4 Stability map for gain k_2, proportional to $\dot{\Phi}$. The region in red represents where there is energy absorbtion in a cycle and the regions in blue where there is energy dissipation.

With that, it is possible to determine the minimum gain of a feedback controller in order to stabilize the effect. One has to keep in mind, however, that simply setting the value to its minimum ideally creates a situation where the initial perturbation is never damped. Considering simulation

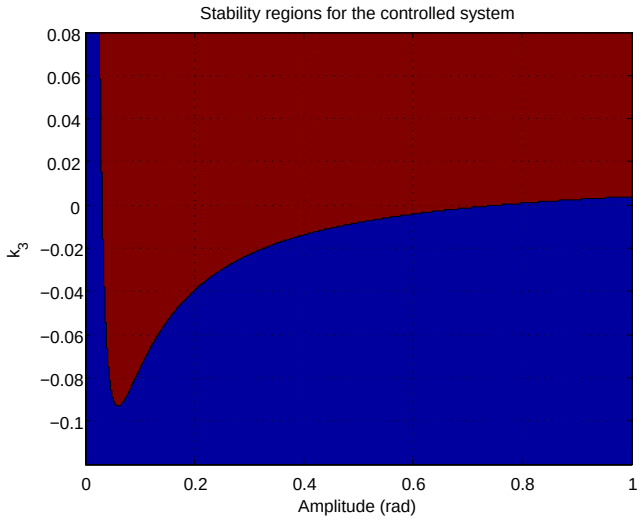

Fig. 5 Stability map for varying values of k_3

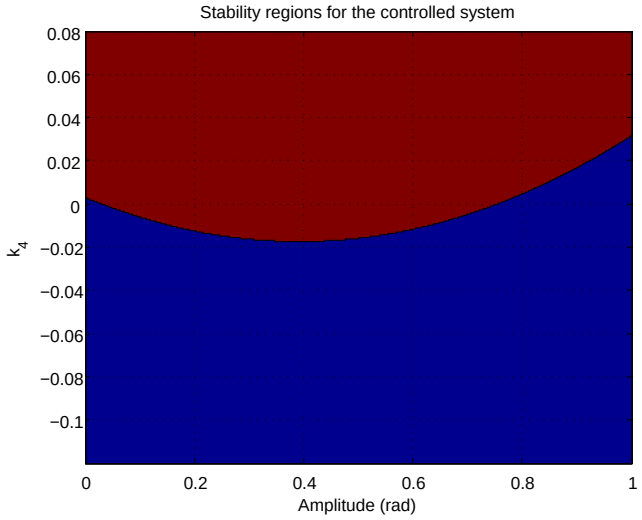

Fig. 6 Stability map for gain k_4

and precision errors, choosing a value that is too close to the minimum necessary to keep stability creates a situation similar to that seen in Fig. 2, where an initial perturbation takes a long time to be damped.

Another method to analyze the stability of the loop that is redundant in this case, but it is necessary in cases where the integration cannot be evaluated analytically. This method consists in setting a value for k and sweeping values of A. This is represented in the stability maps in Figs. 4 to 6.

It is also important to note in these maps the representation of the existence of a limit-cycle oscillation. That is the case where an horizontal line (constant k) intercepts the neutral line. The first and the second intersection represent the critical initial perturbation and the LCO amplitude, respectively.

4.1 Testing of the methodology using an on-off controller activated by a thresold

Another control law model that can be exploited is that of an on-off controller that acts against the roll rate if some angle is exceeded, written as,

$$\begin{aligned} ||\Phi|| > \Phi_{thr} &\Rightarrow C_{l_{\delta_a}} = \tilde{k}_5 \frac{\dot{\Phi}}{||\dot{\Phi}||} \\ ||\Phi|| < \Phi_{thr} &\Rightarrow C_{l_{\delta_a}} = 0 \end{aligned} \tag{25}$$

This control law can represent the asymmetrical activation of a spoiler to counteract roll motion added to a derivative action. It is possible to solve this equation in a numerical form, using the arguments in Eq. (16) and also

$$\begin{aligned} \Phi_{thr} &= 10^\circ \\ \tilde{k}_2 &< 0 \\ \tilde{k}_5 &= -0.3 \end{aligned} \tag{26}$$

It is evident that this problem could be solved analytically, by dividing the integration in the discontinuity. However, the numerical method is proposed in order to exemplify the application with a hypothetical rule that is not analytically solvable.

The first step is to create a time vector and calculate the imposed Φ and $\dot{\Phi}$.

$$\begin{aligned} \vec{t} &= 0 : step : \frac{2\pi}{\tilde{\omega}_n} \\ \vec{\Phi} &= sin(\vec{t}) \\ \vec{\dot{\Phi}} &= cos(\vec{t}) \end{aligned} \tag{27}$$

Then the moment of each term of the equation is

$$\begin{aligned} \vec{L_1} &= a_1 A\vec{\Phi} \\ \vec{L_2} &= a_2 A\vec{\dot{\Phi}} \\ \vec{L_3} &= a_3 A\vec{\Phi}|A\vec{\dot{\Phi}}| \\ \vec{L_4} &= a_4 \frac{A\vec{\dot{\Phi}}}{|A\vec{\dot{\Phi}}|} \end{aligned} \tag{28}$$

$$\vec{L_5} = ||\Phi|| > \Phi_{thr} \Rightarrow C_{l_{\delta_a}} = \tilde{k}_5 \frac{A\dot{\Phi}}{||A\dot{\Phi}||}$$
$$||\Phi|| < \Phi_{thr} \Rightarrow C_{l_{\delta_a}} = 0$$

It is then simple to integrate the energy contribution from each term. In this work the trapezoidal rule was used.

The stability map as obtained shown in Fig. 7, when compared to Fig. 8 shows that the spoiler action is extremely effective in controlling oscillations with high amplitude. In order to assess these results, they are compared to simulation results.

The comparison between numerical simulation is again very precise, with the numerical method predicting 16.4° for $\tilde{k}_2 = -0.05$ while the figure obtained by simulation is 16.2°.

It is important to cite that the simulation result for this case is not stable, in fact the simulation results are completely unreliable after $A = A_{max}$, as in this point naturally $\dot{\Phi}_{A_{max}} = 0$, and then any acceleration will be counteracted by the spoiler. The agreement between the method result and the simulation is again not explained by the authors, and precautions should be taken to avoid this kind of situation.

One proposed solution to obtain reliable simulation results is changing the control law, so that the spoiler is activated if $\Phi > 10^\circ$ and $\dot{\Phi} > 5^\circ/s$.

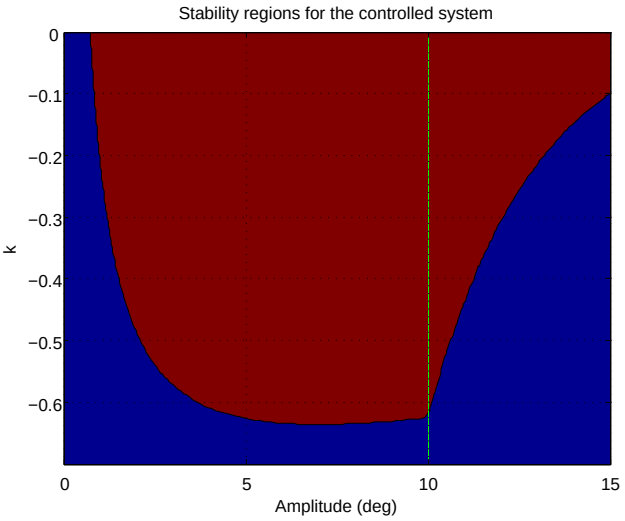

Fig. 7 Stability map for them problem using a derivative controller and a the actuation of spoilers if the amplitude is greater than 10°

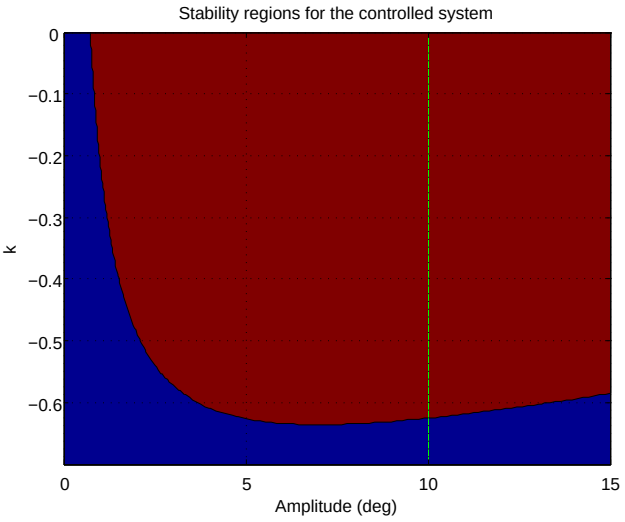

Fig. 8 Stability map of the same problem without the action of the spoiler

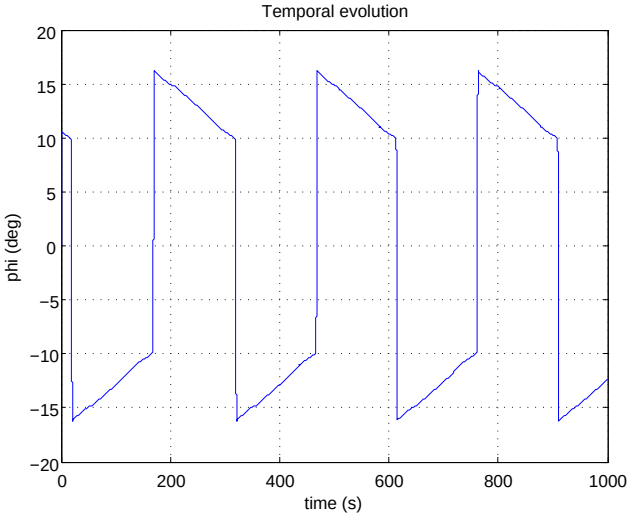

Fig. 9 Simulation results for control using asymmetric spoiler activation. Note that after achieving maximum amplitude, the simulation becomes unstable, as any movement is counteracted by the spoiler. In fact, the time spent on the region where $\Phi > 10^\circ$ is only dependent on the simulation timestep.

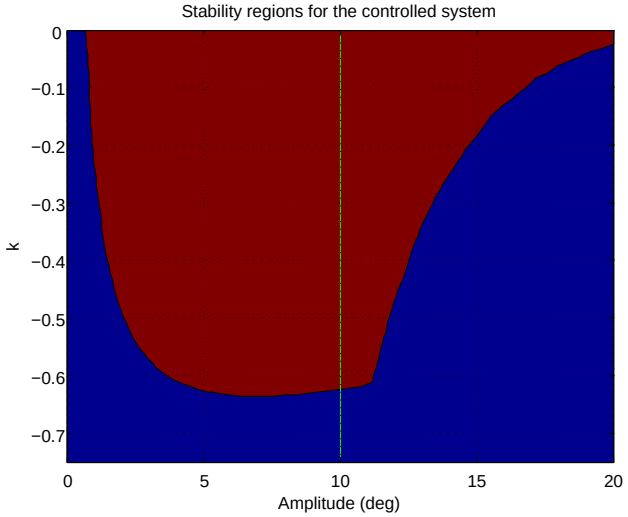

Fig. 10 Stability map for controller using asymmetrical spoiler after a threshold of position and rate. Note that the maximum value of the controller gain for the system to be stable is dependent only on the behavior of the system before the position threshold (green line).

This renders the simulation stable and independent of the time step. Comparing again the result on the stability map (that is slightly changed due to the new dead zone) for the same $\tilde{k}_2 = -0.05$, one obtains a predicted amplitude of 18.6° and a measured amplitude of 18.0° , a margin that is considered satisfactory for this application.

The stability map for this situation is shown in Fig. 10. The final important conclusion about this analysis is that the absolute stability limit is not changed, as the highest value for $\tilde{k}_2$ that guarantees stability for any initial perturbation is under the region where the spoiler is activated.

5 Conclusion

The present work has proposed a method for determining the stability limits for non-linear single degree of freedom models with and without a controller, applied to the analysis of the wing rock phenomenon.

Results from simulations have been compared to those obtained by the procedure usually shows good agreement (in the order of magnitude of 1%), and yield some precision even when one of the hypothesis is not verified, namely, that the LCO is approximately by harmonic motion.

The method, while extremely simplified for wing rock motion, and does not allow predicting of the phenomenon, only works in a model that represents an airplane undergoing the phenomenon, could also be used in other fields of engineering where single degree of freedom LCO are concerned.

Acknowledgements

The authors would like to thank the Brazilian Reseach Agency, CNPq, and the Engineering School of São Carlos of the University of São Paulo for financing the presentation of this work.

References

[1] J. Katz, “Wing vortex interactions and wing rock,” *Progress in Aerospace Science*, vol. 35, pp. 727–750, 1999.

[2] R. C. Nelson and A. Pelletier, "The unsteady aerodynamics of slender wings and aircraft undergoing large amplitude maneuvers," *Prog. in Aerosp. Sci.*, vol. 39, pp. 185–248, 2003.

[3] C. Hwang and W. S. Pi, "Investigation of steady and fluctuating pressures associated with the transonic buffeting and wing rock of a one-seventh scale model of the F-5A aircraft," tech. rep., NASA CR-3061, 1978.

[4] R. C. Monaghan and E. L. Friend, "Effects of flaps on buffet characteristics and wing-rock onset of an F-8C airplane at subsonic and transonic speeds," tech. rep., NASA TM X-2873, 1973.

[5] B. S. Liebst, "The dynamics, prediction, and control of wing rock in high-performance aircraft," *Phil. Trans. R. Soc. Lond.*, p. 2257, 1998.

[6] A. A. Saad, *Simulation and analysis of wing rock physics for a generic fighter model with three degrees-of-freedom*. PhD thesis, Air Force Institute of Technology, 2000.

[7] G. Guglieri and F. Quagliotti, "Experimental observation and discussion of the wing rock phenomenom," *Aerosp. Sci. Technol.*, vol. 2, pp. 111–123, 1995.

[8] G. Guglieri and F. B. Quagliotti, "Analytical and experimental analysis of wing rock," *Nonlinear Dynamics*, vol. 24, pp. 129–146, 2001.

Copyright Statement